

HEAT TRANSFER IN A PACKED BED OF ADSORBENTS BY PULSE RESPONSE

AKIYOSHI SAKODA AND MOTOYUKI SUZUKI

Institute of Industrial Science, University of Tokyo, Tokyo 106

Key Words: Heat Transfer, Mass Transfer, Adsorption, Axial Dispersion, Heat Pulse Response

Heat transfer in a packed bed of adsorbents is influenced by mass transfer due to adsorption/desorption. As the first step to clarify this phenomenon, axial heat transfer in a packed bed of silica-gel in dynamic equilibrium with air flow containing water vapor was investigated. Moments of heat pulse response curves were employed for the analysis. The first absolute moment and the second central moment were derived theoretically from a model taking into account mass transfer due to adsorption and the axial dispersion of an adsorbable component in the bed. Also, heat pulse responses were experimentally obtained for three levels of water vapor concentrations. Their moments could be appropriately accounted for by the theoretical treatment adopted here. A simplified heat transfer model could be used by defining the apparent parameters including the effects of mass transfer due to adsorption.

1. Introduction

In commercial adsorption operations there are many cases, such as adiabatic adsorption and thermal regenerations, where it is important to take into account heat transfer in a packed bed of adsorbents. Heat transfer in such beds is considered to be directly affected by the transport of adsorbate, since the adsorption equilibrium relation depends on temperature and adsorption/desorption is accompanied by the giving/receiving of heat of adsorption to/from adsorbents. Mechanisms of heat transfer associated with the adsorption phenomenon, however, have not yet been established theoretically or even experimentally. In this work, as the first step to clarify the problem, the axial heat transfer in a packed bed of silica-gel in dynamic equilibrium with air flow containing water vapor is investigated by the heat pulse response method. The first absolute moment and the second central moment of heat pulse responses in the adsorption column are deduced theoretically and are also experimentally examined. To make clear the effect of adsorption on heat transfer, typical response curves obtained experimentally are shown in Fig. 1. Response curve (I) was obtained in a case where no adsorbable component existed in the carrier stream. Response curve (II) was obtained in a case where the adsorbent was in dynamic equilibrium with the flowing gas which contains moisture. The flow rate of the flowing gas in the two cases is almost the same, as shown in Fig. 1. It is obvious that there is a considerable difference between the two curves. The purpose of this work is to give a quantitative interpretation of

the difference between the cases where adsorption/desorption takes place and where it does not.

2. Theory

2.1 Fundamental Equations

The adsorption system which is the object of this work is composed of silica-gel for adsorbent, water vapor for adsorbate and air for the carrier gas. This system is often found in operations to lower humidity in an air stream. In these operations, the flow rate of air in the adsorption column is usually in the low Reynolds number region. Then temperature difference between particle and fluid is not considered in the analysis model used in this work.⁷⁾ Since adsorption rate in this system is controlled by surface diffusion inside the adsorbent particle,¹⁾ resistance of fluid film to mass transfer between particle and fluid is not taken into account. Then the fundamental equations are given as follows.

The heat balance in the bed is expressed as

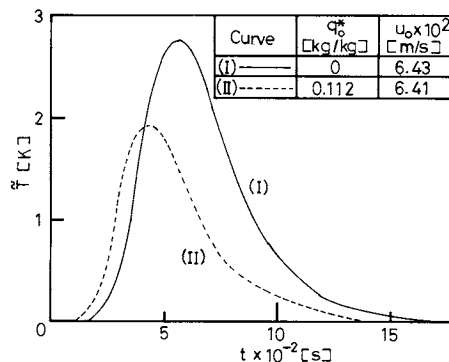


Fig. 1. Typical heat pulse response curves.

Received June 27, 1983. Correspondence concerning this article should be addressed to A. Sakoda.

$$\left(\rho_g C_{pg} + \frac{\gamma}{\varepsilon} C'_{ps}\right) \frac{\partial T}{\partial t} - \frac{k_{ez}}{\varepsilon} \cdot \frac{\partial^2 T}{\partial z^2} + \frac{u_0}{\varepsilon} \rho_g C_{pg} \frac{\partial T}{\partial \tau} - Q \frac{\gamma}{\varepsilon} \frac{\partial q}{\partial t} = 0 \quad (1)$$

where ρ_g is the density of the flowing gas, C_{pg} is the heat capacity of the flowing gas, γ is the packing density, ε is the void fraction, C'_{ps} is the apparent heat capacity of the adsorbent solid, which is expected to vary with the amount adsorbed, k_{ez} is the axial effective thermal conductivity, u_0 is the flow rate of the flowing gas, Q is the heat of adsorption and q is the amount adsorbed.

The mass balance in the bed is written in the same manner as

$$\frac{\partial C}{\partial t} - \frac{E_z}{\varepsilon} \frac{\partial^2 C}{\partial z^2} + \frac{u_0}{\varepsilon} \frac{\partial C}{\partial z} + \frac{\gamma}{\varepsilon} \cdot \frac{\partial q}{\partial t} = 0 \quad (2)$$

where C is the concentration of an adsorbable component in the flowing gas and E_z is the axial dispersion coefficient.

Mass transfer due to adsorption/desorption between adsorbent particle and fluid is expressed as

$$\gamma \frac{\partial q}{\partial t} = k_s a_v (q^* - q) \quad (3)$$

where q^* is the equilibrium amount adsorbed and $k_s a_v$ is the overall mass transfer coefficient.

The adsorption equilibrium relation is expressed in its most simplified form as

$$q^* = K_0 \exp\left(\frac{Q}{RT}\right) C \quad (4)$$

where K_0 is a constant and R is the gas constant.

2.2 Moments of heat pulse response curve

Here with regard to small heat pulses, perturbations of T , C , q and q^* around the dynamic steady condition, where $q_0^* = K_0 \exp(Q/RT_0) C_0$ holds, are considered as follows.

$$\begin{aligned} T &= T_0 + \tilde{T} \\ C &= C_0 + \tilde{C} \\ q &= q_0^* + \tilde{q} \\ q^* &= q_0^* + \tilde{q}^* \end{aligned} \quad (5)$$

Then T , C , q and q^* in Eqs. (1)–(3) are respectively alternated with \tilde{T} , \tilde{C} , \tilde{q} and \tilde{q}^* and the adsorption equilibrium given by Eq. (4) is linearized for both temperature and concentration as

$$\begin{aligned} \tilde{q}^* &= \left(\frac{\partial q^*}{\partial C}\right) \tilde{C} + \left(\frac{\partial q^*}{\partial T}\right) \tilde{T} \\ &= K_0^* \tilde{C} - \frac{K_0^* Q C_0}{RT_0^2} \tilde{T} \end{aligned} \quad (6)$$

where

$$K_0^* = K_0 \exp\left(\frac{Q}{RT_0}\right) \quad (7)$$

Heat pulse responses, $\tilde{T}(t)$, are analyzed by the first absolute moment, μ_1 , and the second central moment, μ_2' , of $\tilde{T}(t)$, since the low-order moment analysis is expected to be useful to quantitatively clarify the effect of mass transfer due to adsorption on heat transfer.

The n -th absolute moment, μ_n , and the n -th central moment, μ_n' , of the heat pulse response are respectively defined as

$$\mu_n \equiv \int_0^\infty t^n \tilde{T} dt / \int_0^\infty \tilde{T} dt \quad (8)$$

and

$$\mu_n' \equiv \int_0^\infty (t - \mu_1)^n \tilde{T} dt / \int_0^\infty \tilde{T} dt \quad (9)$$

The solution of the basic differential equations describing the system in the Laplace domain, $G(p)$, is given by

$$G(p) = \int_0^\infty e^{-pt} \tilde{T} dt / \int_0^\infty \tilde{T} dt \quad (10)$$

Then the following relation is derived from Eqs. (8) and (10).

$$\mu_n = \lim_{p \rightarrow 0} \left(-\frac{\partial}{\partial p}\right)^n G(p) \quad (11)$$

To determine the moments for our system from Eqs. (9)–(11), Laplace transformations of the fundamental equations are carried out by using the following relations.

$$\begin{aligned} \int_0^\infty e^{-pt} \tilde{x} dt &= \bar{x} \\ \int_0^\infty e^{-pt} \frac{\partial^n \tilde{x}}{\partial z^n} dt &= \frac{\partial^n \bar{x}}{\partial z^n} \quad (n=1, 2) \\ \int_0^\infty e^{-pt} \frac{\partial \tilde{x}}{\partial t} dt &= p \bar{x} \end{aligned} \quad (12)$$

where x represents variables such as T , C , q and q^* .

Eliminating \tilde{C} , \tilde{q} and \tilde{q}^* from the Laplace transform of the fundamental equations gives

$$\begin{aligned} k_{ez} \cdot E_z \frac{\partial^4 \bar{T}}{\partial z^4} - u_0 (k_{ez} + E_z \rho_g C_{pg}) \frac{\partial^3 \bar{T}}{\partial z^3} \\ - \left[\varepsilon p \left\{ k_{ez} + E_z \left(\rho_g C_{pg} + \frac{\gamma}{\varepsilon} C'_{ps} \right) \right. \right. \\ \left. \left. + \left(\frac{\gamma}{\varepsilon} \right) \frac{K_0^* k_s a_v \left(k_{ez} + E_z \frac{Q^2 C_0}{RT_0^2} \right)}{\gamma p + k_s a_v} \right\} - u_0^2 \rho_g C_{pg} \right] \frac{\partial^2 \bar{T}}{\partial z^2} \end{aligned}$$

$$\begin{aligned}
& + \left[\varepsilon u_0 p \left\{ 2\rho_g C_{pg} + \frac{\gamma}{\varepsilon} C'_{ps} \right. \right. \\
& + \left. \left. \left(\frac{\gamma}{\varepsilon} \right) \frac{K_0 * k_s a_v \left(\rho_g C_{pg} + \frac{Q^2 C_0}{RT_0^2} \right)}{\gamma p + k_s a_v} \right\} \right] \frac{\partial \bar{T}}{\partial z} \\
& + \left[\varepsilon^2 p^2 \left\{ \rho_g C_{pg} + \frac{\gamma}{\varepsilon} C'_{ps} \right. \right. \\
& + \left. \left. \left(\frac{\gamma}{\varepsilon} \right) \frac{K_0 * k_s a_v \left(\rho_g C_{pg} + \frac{\gamma}{\varepsilon} C'_{ps} + \frac{Q^2 C_0}{RT_0^2} \right)}{\gamma p + k_s a_v} \right\} \right] \bar{T} = 0
\end{aligned} \quad (13)$$

The μ_1 and μ_2' were determined from Eq. (13) by neglecting its first two terms, since these high-order terms are not concerned in either μ_1 or μ_2' .⁶⁾ And then for simplifying the analysis of μ_2' , H is defined as follows.

$$H \equiv \frac{\mu_2'/(2z/u_0)}{\{\mu_1/(z/u_0)\}^2} \quad (14)$$

The resulting expressions for μ_1 and H are given as

$$\mu_1 = \frac{\gamma C'_{ps}}{\rho_g C_{pg} + \frac{Q^2 C_0}{RT_0^2}} \left(\frac{z}{u_0} \right) \quad (15)$$

$$H = \frac{k_{ez} + E_z \frac{Q^2 C_0}{RT_0^2}}{\rho_g C_{pg} + \frac{Q^2 C_0}{RT_0^2}} \cdot \frac{1}{u_0^2} + \frac{\frac{Q^2 C_0}{RT_0^2}}{k_s a_v \cdot K_0 * \left(\rho_g C_{pg} + \frac{Q^2 C_0}{RT_0^2} \right)} \quad (16)$$

(see Appendix)

3. Experimental

3.1 Apparatus

To examine the theoretical consideration developed earlier, experiments of heat pulse responses were carried out as follows. The schematic diagram of experimental apparatus is shown in Fig. 2. Air from a compressor was introduced into a packed bed of silica-gel after the water vapor concentration was controlled. The flow rate was under 7.5×10^{-2} m/s. Details of the packed bed are shown in Fig. 3. Silica-gel particles were packed in a tube of 6×10^{-2} m i.d., made of acrylic resin and wrapped with asbestos sheets. The packing density, γ , was 7.8×10^2 kg/m³. The heater was made of Nichrome wire and designed to give the heat pulse uniformly to a cross section of the bed. Details of the heater are shown in Fig. 4. A CA thermocouple was inserted into the bed at 6.5×10^{-2} m after the heater, perpendicularly to the center axis. The temperature changes with time were recorded on a recorder by amplifying the output of

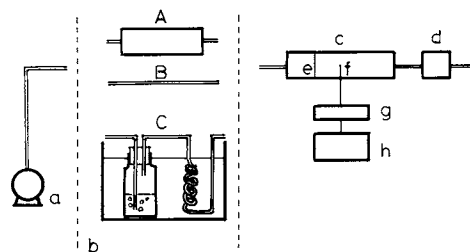


Fig. 2. Schematic diagram of experimental apparatus. a, compressor; b, section for controlling water vapor concentration; c, packed bed of adsorbents; d, gas meter; e, heater; f, thermocouple; g, DC amp.; h, recorder.

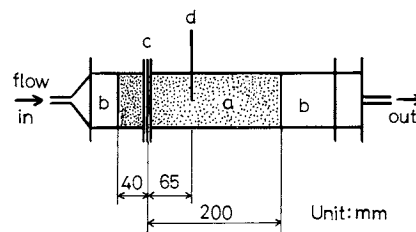


Fig. 3. Details of packed bed of adsorbents. a, silica gel particles; b, glass beads; c, heater; d, CA thermocouple.

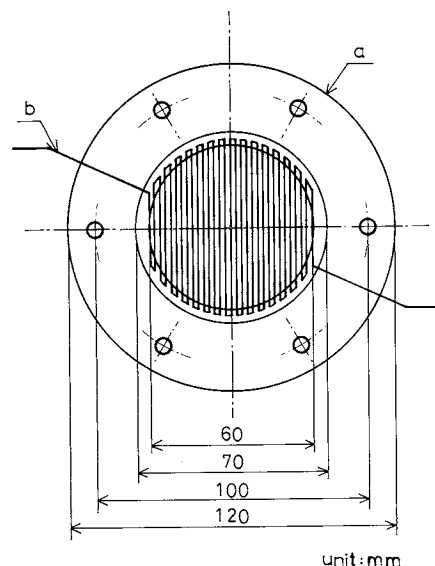


Fig. 4. Details of heater. a, acrylic resin plate; b, nichrome wire.

the thermocouple with a DC amp.

Adsorbent

The adsorbent used in this work was silica-gel A type manufactured by Fuji Davison Co., Ltd. Particles between 6 and 8 mesh size were used. The average diameter of the particle, d_p , was 2.8×10^{-3} m. The adsorption equilibrium of water vapor on this adsorbent at 298 K was measured by the conventional gravimetric method using a quartz balance and the isotherm obtained is shown in Fig. 5. The heat of adsorption, Q , in this system is given as 2.8×10^6 J/kg.⁹⁾

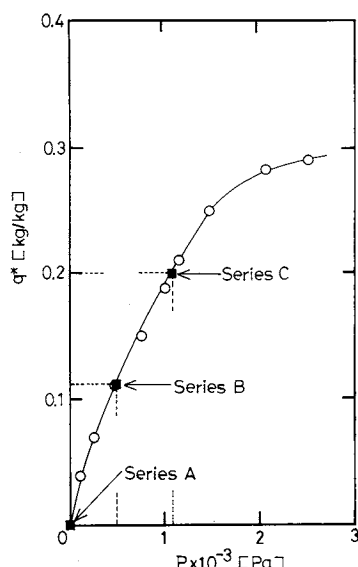


Fig. 5. Adsorption isotherm of water vapor on silica gel A type at 298 K.

Moisture control

Three different methods, shown in Fig. 2 as A, B and C, were employed to prepare three levels of water vapor concentration in the air stream to be introduced into the packed bed of silica-gel.

Series A: Air from a compressor was passed through another silica-gel packed bed of 3.0×10^{-1} m length and 6.0×10^{-2} m i.d., so that the water vapor in the air was completely removed. Thus water vapor concentration in the air introduced into the packed bed, C_0 , was nearly zero.

Series B: The air was directly introduced into the packed bed. By this method, water vapor concentration was kept constant at $C_0 = 3.88 \times 10^{-3}$ kg/m³, since the pressure and temperature in the gas holder of the compressor were kept constant at 6.1×10^5 Pa and 298 K, respectively.

Series C: The air was passed through pure water at a constant temperature of 292 K. By this method, air containing moisture of $C_0 = 8.24 \times 10^{-3}$ kg/m³ was generated.

The constancy of C_0 was checked by a hygrometer (Panametric) and no change was detected regardless of the flow rate of air in our experimental range. Partial pressures of water vapor in the flowing air controlled by these methods and the amounts adsorbed which are equilibrated to them are also shown in Fig. 5. Also, parameters describing the dynamic steady conditions in Series A, B and C are listed in Table 1.

3.2 Procedure

While the experiment was being carried out, the temperature in the laboratory was kept constant at 298 K. The air, the water vapor concentration in which was kept at a constant level by the method

Table 1. Experimental conditions in water vapor and silica gel A type system

Series		A	B	C
C_0	[kg/m ³]	0	3.88×10^{-3}	8.24×10^{-3}
q_0^*	[kg/kg]	0	0.112	0.200
K_0^*	[m ³ /kg]	—	28.9	24.3
$\frac{Q^2 C_0}{RT_0^2}$	[J/(m ³ ·K)]	0	8.44×10^2	1.79×10^3
$\rho_g C_{pg} + \frac{Q^2 C_0}{RT_0^2}$	[J/(m ³ ·K)]	1.19×10^3	2.03×10^3	2.98×10^3

previously described, was passed through the packed bed of silica-gel for over 24 h to bring the adsorbent column into dynamic adsorption equilibrium with the flowing gas. Heat pulses were introduced by the heater when the maximum temperature peak was kept within three degrees by controlling the electric power supply to the heater. The heat pulse responses were measured in the range of flow rate, $u_0 = 2.4\text{--}7.5 \times 10^{-2}$ m/s. From response curves, the first absolute moment, μ_1 , and the second central moment, μ_2' , were calculated by numerical integration according to their definitions in Eqs. (8) and (9).

4. Results and Discussion

4.1 First moment analysis

According to Eq. (15), the slope of μ_1 versus z/u_0 plots means $\gamma C'_{ps}/(\rho_g C_{pg} + Q^2 C_0/RT_0^2)$. Therefore, μ_1 's obtained by the experiments in Series A, B and C are plotted against z/u_0 in Fig. 6. From Fig. 6, the values of C'_{ps} were determined as $C'_{ps} = 1.05 \times 10^3$ J/(kg·K) for Series A, $C'_{ps} = 1.51 \times 10^3$ J/(kg·K) for Series B and $C'_{ps} = 1.89 \times 10^3$ J/(kg·K) for Series C. The dependency of C'_{ps} on the dynamic equilibrium amount adsorbed, q_0^* , is shown in Fig. 7. From Fig. 7, the following relation is obtained.

$$C'_{ps} = \alpha + \beta q_0^* \quad (17)$$

The parameter α in Eq. (17) represents the heat capacity of the adsorbent solid, C_{ps} . The resultant value of C_{ps} was 1.05×10^3 J/(kg·K), which is in good agreement with $C_{ps} = 9.24 \times 10^2$ J/(kg·K) in the literature.¹¹⁾ The resultant value of β is 4.2×10^3 J/(kg·K), which is equal to the heat capacity of water in liquid phase. Then the heat capacity of the adsorbent solid in dynamic steady condition is expected to be expressed as

$$C'_{ps} = C_{ps} + C_{ads} \cdot q_0^* \quad (18)$$

where C_{ads} is the heat capacity of the adsorbate in liquid phase.

4.2 Second moment analysis

Neither resistances of fluid film to heat or mass transfer between particle and fluid are taken into

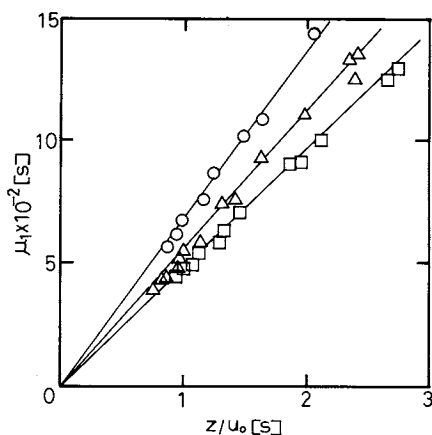


Fig. 6. Dependency of μ_1 on z/u_0 . ○, Series A; △, Series B; □, Series C.

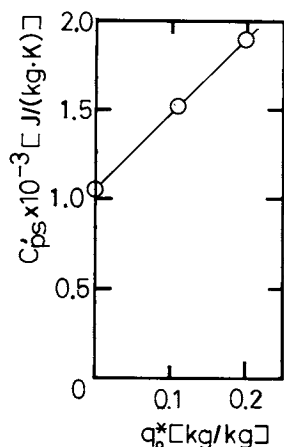


Fig. 7. Dependency of C'_{ps} on q_0^* .

account in this work, as noted earlier. The analysis is carried out by regarding parameters such as k_{ez} and k_e^0 as those in the steady state.

Effect of fluid dispersion

The analysis of μ_2' is carried out by using H defined by Eq. (14). Both the axial effective thermal conductivity, k_{ez} , and the axial dispersion coefficient, E_z , in the first term of H given by Eq. (16) have the contributions of turbulent dispersion in the packed bed. Yagi *et al.*⁽⁸⁾ proposed that k_{ez} be expressed as

$$k_{ez} = k_e^0 + \delta \rho_g C_{pg} d_p u_0 \quad (19)$$

where k_e^0 is the effective thermal conductivity with stagnant fluid, d_p is the diameter of the particle and δ shows the degree of contribution of fluid flow. Similarly, E_z is usually expressed as

$$E_z = \frac{\varepsilon}{\tau} D_M + \frac{1}{Pe} d_p u_0 \quad (20)$$

where D_M is the molecular diffusivity, τ is the tortuosity factor of interstitial fluid path and Pe is defined by

$$Pe = \frac{d_p u_0}{D_z} \quad (21)$$

where D_z is the dispersion coefficient due to fluid mixing. Both δ in Eq. (19) and $1/Pe$ in Eq. (20) represent the contribution of dispersion of heat and mass due to fluid mixing. Then as a first approximation, these are considered to be the same and are expressed as

$$\bar{\delta} \equiv \delta = \frac{1}{Pe} \quad (22)$$

Substituting Eqs. (19), (20) and (22) into Eq. (16) gives

$$H = \frac{k_e^0 + \frac{\varepsilon}{\tau} D_M \left(\frac{Q^2 C_0}{RT_0^2} \right)}{\rho_g C_{pg} + \frac{Q^2 C_0}{RT_0^2}} \cdot \frac{1}{u_0^2} + \bar{\delta} d_p \cdot \frac{1}{u_0} + \frac{\frac{Q^2 C_0}{RT_0^2}}{k_s a_v \cdot K_0^* \left(\rho_g C_{pg} + \frac{Q^2 C_0}{RT_0^2} \right)} \quad (23)$$

which is used for the later analyses.

Dry bed runs (Series A)

By putting $C_0 = 0$ into Eq. (23), H is given as

$$H = \frac{k_e^0}{\rho_g C_{pg}} \cdot \frac{1}{u_0^2} + \bar{\delta} d_p \cdot \frac{1}{u_0} \quad (23')$$

Multiplying Eq. (23)' by u_0 gives

$$u_0 H = \frac{k_e^0}{\rho_g C_{pg}} \cdot \frac{1}{u_0} + \bar{\delta} d_p \quad (23'')$$

According to Eq. (23)'', the slope and the intercept at $1/u_0 = 0$ of $u_0 H$ versus $1/u_0$ plots means $k_e^0 / \rho_g C_{pg}$ and $\bar{\delta} d_p$ respectively. Therefore, $u_0 H$'s obtained by experiment are plotted against $1/u_0$ in Fig. 8. The values of H experimentally obtained vary in the range shown in Fig. 8, since the values of μ_2' derived from response curves vary about 10% owing to the disposal of tails of the curves. The values of k_e^0 and $\bar{\delta}$ were determined from Fig. 8 as $1.5\text{--}2.2 \times 10^{-1} \text{ W/(m} \cdot \text{K)}$ and 0.35–0.7 respectively. This value of k_e^0 is the same order of magnitude as that estimated by the model proposed by Kunii *et al.*⁽⁴⁾ as follows:

$$\frac{k_e^0}{k_{fl}} = \varepsilon + \frac{1 - \varepsilon}{\phi + \left(\frac{2}{3} \right) \left(\frac{k_{fl}}{k_{so}} \right)} \quad (24)$$

where k_{fl} is the thermal conductivity of fluid, k_{so} is that of the solid and ϕ is a ratio of fluid thickness between two adjacent packings to diameter of the particle. The resultant value of $\bar{\delta}$ is considered to be reasonable in comparison with those in the literature, such as 0.7–0.8,⁽⁸⁾ 0.55–0.7⁽⁵⁾ and 0.5.⁽³⁾

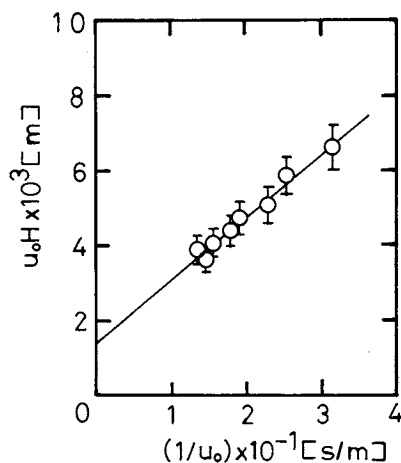


Fig. 8. $u_0 H$ versus $1/u_0$ plots.

Adsorption runs (Series B and C)

The term $(\varepsilon/\tau)D_M(Q^2C_0/RT_0^2)$ in Eq. (23) is found to be negligible, since the values of $(\varepsilon/\tau)D_M(Q^2C_0/RT_0^2)$ evaluated by using $D_M = 2.56 \times 10^{-5} \text{ m}^2/\text{s}$, $\varepsilon = 0.4$, $\tau = 1-2$ and parameters describing our experimental conditions are at least one order of magnitude smaller than that of k_e^0 determined earlier. The Eq. (23) is reduced to Eq. (25).

$$H = \frac{k_e^0}{\rho_g C_{pg} + \frac{Q^2 C_0}{RT_0^2}} \cdot \frac{1}{u_0^2} + \delta d_p \frac{1}{u_0} + \frac{\frac{Q^2 C_0}{RT_0^2}}{k_s a_v \cdot K_0 * \left(\rho_g C_{pg} + \frac{Q^2 C_0}{RT_0^2} \right)} \quad (25)$$

According to Eq. (25), H 's obtained by experiment in Series B are plotted against $1/u_0$ in Fig. 9. The first and second terms of Eq. (25) were calculated by using the average k_e^0 and δ determined from Fig. 8 and the sum of the two are also shown in Fig. 9 by a dashed line. By fitting a line paralleling the dashed line to experimental results, the third term of Eq. (25), which is the intercept at $1/u_0 = 0$ in Fig. 9, was determined. Then $k_s a_v$ was evaluated as $0.48-1.4 \text{ kg}/(\text{m}^3 \cdot \text{s})$. The same procedure is tried for the results from Series C in Fig. 10. Then $k_s a_v$ was evaluated as $0.59-1.1 \text{ kg}/(\text{m}^3 \cdot \text{s})$, which is in good agreement with the values obtained from Series B. Here the propriety of the values of $k_s a_v$ determined above is discussed. In a case where surface diffusion inside the adsorbent particle is the controlling step of mass transfer, $k_s a_v$ is given by²⁾

$$k_s a_v \approx \frac{60\gamma D_s}{d_p^2} \quad (26)$$

where D_s is the surface diffusivity in the particle. The value of $k_s a_v$ evaluated by Eq. (26) with $D_s = 0.6-$

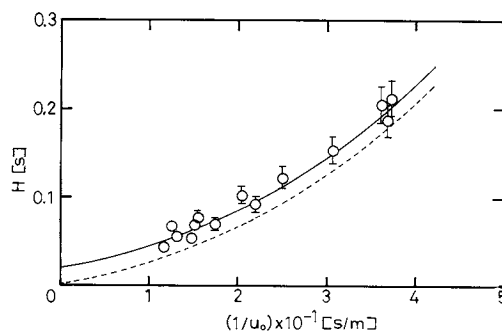


Fig. 9. Dependency of H on $1/u_0$ in Series B.

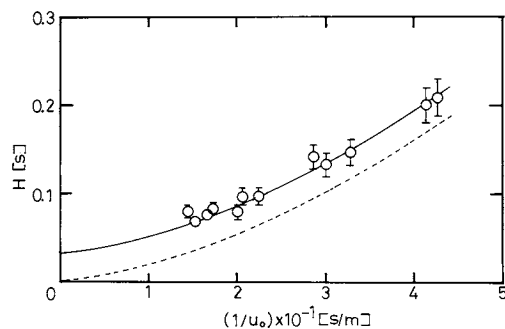


Fig. 10. Dependency of H on $1/u_0$ in Series C.

$3 \times 10^{-10} \text{ m}^2/\text{s}$ ¹²⁾ is $0.4-1.8 \text{ kg}/(\text{m}^3 \cdot \text{s})$. Thus our resultant values are found to be reasonable, and the experimental results are appropriately accounted for by the model proposed in this work.

4.3 Apparent parameters in simplified treatment

Apparent parameters including the effects of adsorption are considered for the simplified treatment. Equations (15) and (16) with $C_0 = 0$ are respectively given as

$$\mu_1 = \frac{\gamma C_{ps}}{\rho_g C_{pg}} \cdot \frac{z}{u_0} \quad (27)$$

and

$$H = \frac{k_{ez}}{\rho_g C_{pg}} \cdot \frac{1}{u_0^2} \quad (28)$$

Then μ_1 and H with the effect of adsorption are expressed in the same forms as Eqs. (27) and (28) by using apparent parameters.

$$\mu_1 = \frac{\gamma(C_{ps})_{app}}{(\rho_g C_{pg})_{app}} \cdot \frac{z}{u_0} \quad (29)$$

$$H = \frac{(k_{ez})_{app}}{(\rho_g C_{pg})_{app}} \cdot \frac{1}{u_0^2} \quad (30)$$

Comparisons between Eqs. (15) and (29) and between Eqs. (16) and (30) give the apparent parameters in the above expressions as follows.

$$(C_{ps})_{app} = C_{ps} + C_{ads} \cdot q_0^* \quad (18)$$

$$(\rho_g C_{pg})_{app} = \rho_g C_{pg} + \frac{Q^2 C_0}{RT_0^2} \quad (31)$$

$$(k_{ez})_{app} = k_{ez} + \left(E_z + \frac{u_0^2}{k_s a_v \cdot K_0^*} \right) \left(\frac{Q^2 C_0}{RT_0^2} \right) \quad (32)$$

5. Conclusion

Heat transfer in a packed bed of adsorbents is influenced by mass transfer due to adsorption/desorption, since the adsorption equilibrium relation depends on temperature and adsorption/desorption is accompanied by the giving/receiving of heat of adsorption. In this work, as the first step to clarify the effects of the transport of adsorbate on heat transfer, the axial heat transfer in a packed bed of silica-gel in dynamic equilibrium with air flow containing water vapor was investigated by the moment analysis of the heat pulse response. The first absolute moment and the second central moment of this system were derived theoretically from a model that takes into account mass transfer due to adsorption/desorption and dispersions of heat and mass due to fluid mixing.

$$\begin{aligned} \mu_1 &= \frac{\gamma C'_{ps}}{\rho_g C_{pg} + \frac{Q^2 C_0}{RT_0^2}} \cdot \frac{z}{u_0} \\ H &\equiv \frac{\mu_2' / (2z / u_0)}{\{\mu_1 / (z / u_0)\}^2} \\ &= \frac{k_e^0 + \frac{\varepsilon}{\tau} D_M \left(\frac{Q^2 C_0}{RT_0^2} \right)}{\rho_g C_{pg} + \frac{Q^2 C_0}{RT_0^2}} \cdot \frac{1}{u_0^2} + \bar{\delta} d_p \cdot \frac{1}{u_0} \\ &\quad + \frac{\frac{Q^2 C_0}{RT_0^2}}{k_s a_v \cdot K_0^* \left(\rho_g C_{pg} + \frac{Q^2 C_0}{RT_0^2} \right)} \end{aligned}$$

Experimental results were appropriately accounted for by the model proposed here. The apparent parameters including the effects of adsorption were derived from the model as follows.

$$(C_{ps})_{app} = C_{ps} + C_{ads} \cdot q_0^*$$

$$\begin{aligned} \mu_2' &= \frac{2z}{u_0^3 \rho_g C_{pg}} \left\{ \varepsilon k_{ez} + \varepsilon E_z \left(\rho_g C_{pg} + \frac{\gamma}{\varepsilon} C'_{ps} \right) + \gamma K_0^* \left(k_{ez} + E_z \frac{Q^2 C_0}{RT_0^2} \right) \right\} \cdot \left\{ \frac{\varepsilon^2 \left(\rho_g C_{pg} + \frac{\gamma}{\varepsilon} C'_{ps} \right) + \varepsilon \gamma K_0^* \left(\rho_g C_{pg} + \frac{Q^2 C_0}{RT_0^2} + \frac{\gamma}{\varepsilon} C'_{ps} \right)}{B} \frac{A-B}{2\rho_g C_{pg}} \right\} \\ &\quad + \frac{2z\gamma^2 K_0^*}{u_0 \cdot k_s a_v \cdot B} \left\{ \varepsilon \left(\rho_g C_{pg} + \frac{Q^2 C_0}{RT_0^2} + \frac{\gamma}{\varepsilon} C'_{ps} \right) - \frac{\left(\rho_g C_{pg} + \frac{Q^2 C_0}{RT_0^2} \right) (A-B)}{2\rho_g C_{pg}} \right\} \end{aligned} \quad (A-7)$$

where

$$A = \varepsilon \left(2\rho_g C_{pg} + \frac{\gamma}{\varepsilon} C'_{ps} \right) + \gamma K_0^* \left(\rho_g C_{pg} + \frac{Q^2 C_0}{RT_0^2} \right) \quad (A-8)$$

$$\begin{aligned} (\rho_g C_{pg})_{app} &= \rho_g C_{pg} + \frac{Q^2 C_0}{RT_0^2} \\ (k_{ez})_{app} &= k_{ez} + \left(E_z + \frac{u_0^2}{k_s a_v \cdot K_0^*} \right) \left(\frac{Q^2 C_0}{RT_0^2} \right) \end{aligned}$$

The above expressions clearly show the effect of adsorption on heat transfer. Thus in the system adopted in this work there were considerable effects of adsorption on heat transfer. In other systems there may be similar effects in more complicated forms, and they will be clarified theoretically to establish thermal treatments in adsorption operations.

Appendix

Neglecting the first two terms of Eq. (13) gives

$$a(p) \frac{\partial^2 \bar{T}}{\partial z^2} + b(p) \frac{\partial \bar{T}}{\partial z} + c(p) \bar{T} = 0 \quad (A-1)$$

where

$$\begin{aligned} a(p) &= -\varepsilon p \left\{ k_{ez} + E_z \left(\rho_g C_{pg} + \frac{\gamma}{\varepsilon} C'_{ps} \right) \right. \\ &\quad \left. + \left(\frac{\gamma}{\varepsilon} \right) \frac{K_0^* k_s a_v \left(k_{ez} + E_z \frac{Q^2 C_0}{RT_0^2} \right)}{\gamma p + k_s a_v} \right\} - u_0^2 \rho_g C_{pg} \end{aligned} \quad (A-2)$$

$$b(p) = \varepsilon u_0 p \left\{ 2\rho_g C_{pg} + \frac{\gamma}{\varepsilon} C'_{ps} + \left(\frac{\gamma}{\varepsilon} \right) \frac{K_0^* k_s a_v \left(\rho_g C_{pg} + \frac{Q^2 C_0}{RT_0^2} \right)}{\gamma p + k_s a_v} \right\} \quad (A-3)$$

$$\begin{aligned} c(p) &= \varepsilon^2 p^2 \left\{ \rho_g C_{pg} + \frac{\gamma}{\varepsilon} C'_{ps} \right. \\ &\quad \left. + \left(\frac{\gamma}{\varepsilon} \right) \frac{K_0^* k_s a_v \left(\rho_g C_{pg} + \frac{\gamma}{\varepsilon} C'_{ps} + \frac{Q^2 C_0}{RT_0^2} \right)}{\gamma p + k_s a_v} \right\} \end{aligned} \quad (A-4)$$

Then $G(p)$ defined by Eq. (10) is obtained as

$$G(p) = \exp \left[\frac{-b(p) - \sqrt{\{b(p)\}^2 - 4a(p) \cdot c(p)}}{2a(p)} \right] \quad (A-5)$$

According to Eqs. (11) and (9), μ_1 and μ_2' are determined as

$$\mu_1 = \frac{A-B}{2\rho_g C_{pg}} \cdot \frac{z}{u_0} \quad (A-6)$$

and

$$B = \sqrt{A^2 - 4\rho_g C_{pg} \left\{ \varepsilon^2 \left(\rho_g C_{pg} + \frac{\gamma}{\varepsilon} C'_{ps} \right) + \varepsilon \gamma K_0^* \left(\rho_g C_{pg} + \frac{Q^2 C_0}{RT_0^2} + \frac{\gamma}{\varepsilon} C'_{ps} \right) \right\}} \quad (\text{A-9})$$

Eq. (A-6) is transformed to Eq. (A-10) and H defined by Eq. (14) is obtained as Eq. (A-11).

$$\mu_1 = \frac{2 \left\{ \varepsilon^2 \left(\rho_g C_{pg} + \frac{\gamma}{\varepsilon} C'_{ps} \right) + \varepsilon \gamma K_0^* \left(\rho_g C_{pg} + \frac{Q^2 C_0}{RT_0^2} + \frac{\gamma}{\varepsilon} C'_{ps} \right) \right\}}{A + B} \cdot \frac{z}{u_0} \quad (\text{A-10})$$

$$H = \frac{\varepsilon \left\{ k_{ez} + E_z \left(\rho_g C_{pg} + \frac{\gamma}{\varepsilon} C'_{ps} \right) \right\} + \gamma K_0^* \left(k_{ez} + E_z \frac{Q^2 C_0}{RT_0^2} \right)}{B} \cdot \frac{1}{u_0^2} + \frac{\varepsilon^2 \gamma^2 K_0^* (A + B) \left(\frac{\gamma}{\varepsilon} C'_{ps} \right) \left[\left\{ \frac{\gamma}{\varepsilon} C'_{ps} \left(\frac{3Q^2 C_0}{RT_0^2} - \rho_g C_{pg} \right) - \left(\rho_g C_{pg} + \frac{Q^2 C_0}{RT_0^2} \right) \right\}^2 \right.}{4k_s a_v B \left\{ \varepsilon^2 \left(\rho_g C_{pg} + \frac{\gamma}{\varepsilon} C'_{ps} \right) + \varepsilon \gamma K_0^* \left(\rho_g C_{pg} + \frac{Q^2 C_0}{RT_0^2} + \frac{\gamma}{\varepsilon} C'_{ps} \right) \right\}^2} \\ \times \left(\rho_g C_{pg} - \frac{Q^2 C_0}{RT_0^2} \right) \left\{ \gamma K_0^* + \left(\rho_g C_{pg} - \frac{Q^2 C_0}{RT_0^2} + \frac{\gamma}{\varepsilon} C'_{ps} \right) B + \varepsilon \left(\frac{\gamma}{\varepsilon} C'_{ps} \right) \left(\rho_g C_{pg} - \frac{Q^2 C_0}{RT_0^2} + \frac{\gamma}{\varepsilon} C'_{ps} \right) \right\} \\ \left. \times \left\{ \left(\rho_g C_{pg} + \frac{Q^2 C_0}{RT_0^2} \right) \gamma K_0^* + B \right\} \right] \quad (\text{A-11})$$

Here $(\gamma/\varepsilon)C'_{ps}$ is usually far larger than $\rho_g C_{pg}$,

$$\frac{\gamma}{\varepsilon} C'_{ps} \gg \rho_g C_{pg} \quad (\text{A-12})$$

Numerical estimation using the values listed in Table 1 for our experimental conditions gives

$$\frac{\gamma}{\varepsilon} C'_{ps} \gg \frac{Q^2 C_0}{RT_0^2} \quad (\text{A-13})$$

$$K_0^* \gg 1 \quad (\text{A-14})$$

By applying the above approximations, (A-12)–(A-14), Eqs. (A-10) and (A-11) are reduced as follows.

$$\mu_1 = \frac{2 \cdot \varepsilon \gamma K_0^* \frac{\gamma}{\varepsilon} C'_{ps}}{2 \gamma K_0^* \left(\rho_g C_{pg} + \frac{Q^2 C_0}{RT_0^2} \right)} \cdot \frac{z}{u_0} = \frac{\gamma C'_{ps}}{\rho_g C_{pg} + \frac{Q^2 C_0}{RT_0^2}} \cdot \frac{z}{u_0} \quad (\text{A-15})$$

$$H = \frac{\gamma K_0^* \left(k_{ez} + E_z \frac{Q^2 C_0}{RT_0^2} \right)}{\gamma K_0^* \left(\rho_g C_{pg} + \frac{Q^2 C_0}{RT_0^2} \right)} \cdot \frac{1}{u_0^2} + \frac{\varepsilon^2 \gamma^2 K_0^* \cdot 2 \gamma K_0^* \left(\rho_g C_{pg} + \frac{Q^2 C_0}{RT_0^2} \right) \cdot \frac{\gamma}{\varepsilon} C'_{ps} \cdot 4 \frac{\gamma}{\varepsilon} C'_{ps} \frac{Q^2 C_0}{RT_0^2} \gamma K_0^*}{4k_s a_v \cdot \gamma K_0^* \left(\rho_g C_{pg} + \frac{Q^2 C_0}{RT_0^2} \right) \cdot \left(\varepsilon \gamma K_0^* \cdot \frac{\gamma}{\varepsilon} C'_{ps} \right)^2 \cdot 2 \gamma K_0^* \left(\rho_g C_{pg} + \frac{Q^2 C_0}{RT_0^2} \right)} \\ = \frac{k_{ez} + E_z \frac{Q^2 C_0}{RT_0^2}}{\rho_g C_{pg} + \frac{Q^2 C_0}{RT_0^2}} \cdot \frac{1}{u_0^2} + \frac{\frac{Q^2 C_0}{RT_0^2}}{k_s a_v K_0^* \left(\rho_g C_{pg} + \frac{Q^2 C_0}{RT_0^2} \right)} \quad (\text{A-16})$$

Nomenclature

C	= concentration of an adsorbable component in the flowing gas	[kg/m ³]
C_0	= C in dynamic steady conditions	[kg/m ³]
\bar{C}	= defined by Eq. (5)	[kg/m ³]
\bar{C}	= defined by Eq. (12)	[kg · s/m ³]
C_{ads}	= heat capacity of adsorbate in liquid phase	[J/(kg · K)]
C_{pg}	= heat capacity of the flowing gas	[J/(kg · K)]
C_{ps}	= heat capacity of the adsorbent solid	[J/(kg · K)]
C'_{ps}	= apparent C_{ps}	[J/(kg · K)]
d_p	= average diameter of particle	[m]
D_M	= molecular diffusivity	[m ² /s]
D_s	= surface diffusivity	[m ² /s]

D_z	= dispersion coefficient due to fluid mixing	[m ² /s]
E_z	= axial dispersion coefficient	[m ² /s]
H	= defined by Eq. (14)	[s]
k_{ez}	= axial effective thermal conductivity	[W/(m · K)]
k_e^0	= effective thermal conductivity with stagnant fluid	[W/(m · K)]
k_{fl}	= thermal conductivity of fluid	[W/(m · K)]
k_{so}	= thermal conductivity of solid	[W/(m · K)]
$k_s a_v$	= overall mass transfer coefficient	[kg/(m ³ · s)]
K_0	= pre-exponent constant in Eq. (4)	[m ³ /kg]
K_0^*	= defined by Eq. (7)	[m ³ /kg]
P	= pressure	[Pa]
p	= Laplace variable	[s ⁻¹]
Pe	= defined by Eq. (21)	[—]

q	= amount adsorbed	[kg/kg]
q_0	= q in dynamic steady conditions ($= q_0^*$)	[kg/kg]
\bar{q}	= defined by Eq. (5)	[kg/kg]
\bar{q}	= defined by Eq. (12)	[kg·s/kg]
q^*	= equilibrium amount adsorbed	[kg/kg]
q_0^*	= q^* in dynamic steady conditions	[kg/kg]
\bar{q}^*	= defined by Eq. (5)	[kg/kg]
\bar{q}^*	= defined by Eq. (12)	[kg·s/kg]
Q	= heat of adsorption	[J/kg]
R	= gas constant	[J/(kg·K)]
t	= time	[s]
T	= temperature	[K]
T_0	= T in dynamic steady conditions	[K]
\bar{T}	= defined by Eq. (5)	[K]
\bar{T}	= defined by Eq. (12)	[K·s]
u_0	= flow rate of the flowing gas	[m/s]
z	= distance in axial direction	[m]
α	= constant in Eq. (17)	[J/(kg·K)]
β	= constant in Eq. (17)	[J/(kg·K)]
γ	= packing density	[kg/m ³]
δ	= constant in Eq. (19)	[—]
$\bar{\delta}$	= defined by Eq. (22)	[—]
ε	= void fraction	[—]
μ_n	= n -th absolute moment	[s ^{n}]
μ_n'	= n -th central moment	[s ^{n}]

ρ_g	= density of the flowing gas	[kg/m ³]
τ	= tortuosity factor of interstitial fluid path	[—]
ϕ	= ratio of fluid thickness to diameter of particle	[—]

Literature Cited

- 1) Chihara, K. *et al.*: *J. Chem. Eng. Japan*, in press.
- 2) Gluckauf, E.: *Trans. Faraday Soc.*, **51**, 1540 (1955).
- 3) Ikeda, *et al.*: 3rd Symposium on Reaction Engineering (1963).
- 4) Kunii, D. and J. M. Smith: *AIChE J.*, **6**, 97 (1960).
- 5) Kunii, D. *et al.*: 29th Annual Meeting of Society of Chem. Eng. Japan (1964).
- 6) Suzuki, M.: *J. Chem. Eng. Japan*, **6**, 540 (1973).
- 7) Suzuki, M.: *J. Chem. Eng. Japan*, **8**, 163 (1975).
- 8) Yagi, S., D. Kunii and N. Wakao: *AIChE J.*, **6**, 543 (1960).
- 9) "Chemical Engineering Practice," Vol. 6, p. 306, Butterworths (1958).
- 10) "International Critical Tables," Vol. 5, p. 62, McGraw-Hill (1929).
- 11) The Soc. Chem., Eng., Japan (ed.): "Kagaku Kōgaku Benran (Chem. Engrs. Hand Book)," 4th ed., p. 852, Maruzen (1978).
- 12) The Soc. Chem. Eng., Japan (ed.): "Kagaku Kōgaku Benran (Chem. Engrs. Hand Book)," 4th ed., p. 863, Maruzen (1978).

LIQUID-SOLID MASS TRANSFER IN BASKET TYPE THREE-PHASE REACTORS

SHIGEO GOTO AND TAKAO SAITO

Department of Chemical Engineering, Nagoya University, Nagoya 464

Key Words: Mass Transfer, Ion Exchange, Three Phase Reactor, Catalytic Basket Reactor, Stirred Slurry Reactor

Basket type stirred-tank reactors may be useful for three-phase reactions, that is, reactions between dissolved gas and liquid on solid catalysts, because there is no fear of sedimentation of catalyst particles to the bottom even if large, heavy particles are used. This reactor has been used to investigate three-phase systems of desulfurization of dibenzothiophene,⁴⁾ oxidation of phenol^{5,6)} and oxidation of sulfur dioxide.^{2,7)}

Rates of mass transfer from liquid to solid in basket type reactors were measured for liquid-solid system by Suzuki and Kawazoe⁹⁾ and Teshima and Ohashi.¹⁰⁾ The mass transfer coefficients were greater than those in a stirred slurry reactor. On the other hand, when gas was introduced, Pavko *et al.*⁷⁾ found

that the apparent rate constants in basket type reactors were less than those in the liquid-filled reactor and that the inactivity of the catalyst might be due to gas bubbles entrapped inside catalyst baskets. Also, if the screen openings are very narrow, it may be difficult for the liquid to go through the baskets and mass transfer coefficients become smaller.

In this work, to check the effects of gas flow rates, screen openings and locations of baskets on mass transfer coefficients, rates of mass transfer from liquid to solid are measured in batch reactors by using the ion exchange reaction between the resin in the H⁺ form and sodium hydroxide. Mass transfer coefficients in three types of reactors are compared with published correlations.^{3,8,10)}

Received June 17, 1983. Correspondence concerning this article should be addressed to S. Goto. T. Saito is now with Mandam Co. Ltd., Osaka 540.